



CHORUS

This is the accepted manuscript made available via CHORUS. The article has been published as:

Transient superconductivity without superconductivity

Giuliano Chiriacò, Andrew J. Millis, and Igor L. Aleiner

Phys. Rev. B **98**, 220510 — Published 21 December 2018

DOI: [10.1103/PhysRevB.98.220510](https://doi.org/10.1103/PhysRevB.98.220510)

Transient superconductivity without superconductivity

Giuliano Chiriacò,¹ Andrew J. Millis,^{1,2} and Igor L. Aleiner¹

¹*Department of Physics, Columbia University, New York, NY 10027*

²*Center for Computational Quantum Physics, The Flatiron Institute, New York, NY 10010*

(Dated: October 8, 2018)

Recent experiments on K_3C_{60} and layered copper-oxide materials have reported substantial changes in the optical response following application of an intense THz pulse. These data have been interpreted as the stimulation of a transient superconducting state even at temperatures well above the equilibrium transition temperature. We propose an alternative phenomenology based on the assumption that the pulse creates a non-superconducting, though non-equilibrium situation in which the linear response conductivity is negative. The negative conductivity implies that the spatially uniform pre-pulse state is unstable and evolves to a new state with a spontaneous electric polarization. This state exhibits coupled oscillations of entropy and electric charge whose coupling to incident probe radiation modifies the reflectivity, leading to an apparently superconducting-like response **that resembles the data**. **Dependencies** of the reflectivity on polarization and angle of incidence of the probe are predicted and other experimental consequences are discussed.

PACS numbers: 78.47.jg, 05.65.+b, 47.54.+r

There has been substantial interest in the use of intense radiation fields to drive materials into non-equilibrium states [1]. Particular excitement has been generated by reports [2–4] of dramatic changes in the electromagnetic response of K_3C_{60} and layered copper-oxide materials after their exposure to intense THz radiation. The key features of the data are: i) before the application of the pump pulse, the material is in the normal (unbroken symmetry) state; ii) after photo-excitation of the material by the pump, the reflectivity $R(\omega)$ is measured as a function of the frequency ω of a probe field; iii) for some time after the pump excitation, $R(\omega)$ is found to be substantially enhanced at low frequency, see **insets** in Fig. 1. This enhancement has been interpreted in terms of the creation, by the pulse, of a superconducting (SC) state.

Theories proposed to date [5–11] are all based on the premise that the pump pulse changes the interactions and/or structure in a way that enables a transition to a broken symmetry SC state at a temperature much higher than that of the equilibrium transition. In this Letter we point out that the data do not require this interpretation; instead the observations can be understood within a general phenomenology that does not involve SC.

The essence of our model is: i) we argue on general grounds that a non-equilibrium system can exhibit a negative linear response conductivity; ii) in this case the spatially homogeneous state is unstable and evolves to a new state characterized by domains of constant electric field bounded by sheets of charge, Fig. 2a; iii) in the experimentally relevant situation where the non-equilibrium state is produced by a pulse and thereafter evolves with a conserved energy, we show that the system sustains collective modes strongly coupled to incident radiation, leading to the reflectivity curves shown in Fig. 1.

i) Consider the system out of equilibrium. The sample occupies the half space $z > 0$. Pump radiation incident

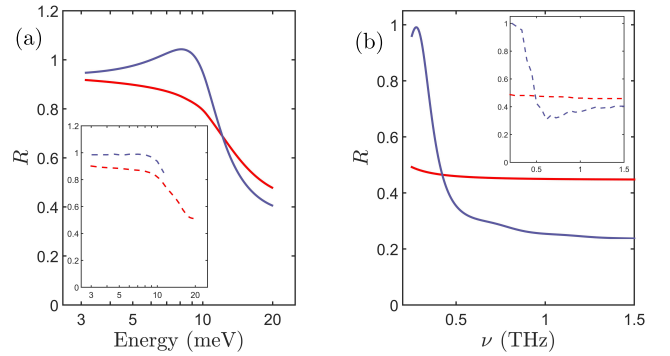


FIG. 1. (Color online) Calculated (solid lines) and experimental (insets, dashed lines) reflectivities for K_3C_{60} (a) and LBCO (b) for equilibrium (red) and non-equilibrium (blue) situations. In panel (a) the data are taken from Fig. 2a of Ref. [2] and the calculations are done as described in the text for angle of incidence $\theta = 45^\circ$ using parameters $\omega_E = 110$ THz, $\gamma = 3.2$ THz, $l_0 = 600$ Å, $\kappa = 3$ cm²s⁻¹. In panel (b) the data are taken from Fig. 2b2 of Ref. [3] and the solid curves are calculated for $\theta = 45^\circ$ using $\omega_E = 1200$ THz, $\gamma = 0.6$ THz, $l_0 = 4500$ Å, $\kappa = 0.2$ cm²s⁻¹. The anisotropy of LBCO was not considered. **The non-equilibrium data of Refs. [2, 3] are processed from raw data and report $R(\omega)$ as if the thickness of the non-equilibrium layer were infinite, thus magnifying the non-equilibrium effects on R ; a direct quantitative comparison with our calculations is not possible, but the resemblance of the curves is very reasonable.**

from $z < 0$ creates a non-equilibrium situation, which we assume relaxes rapidly to a quasi-steady non-equilibrium state; in the simplest case this state is characterized by one parameter, $\zeta(\vec{r}, t)$, which relaxes slowly to its equilibrium value $\zeta = 0$. The precise microscopic description of ζ is not important here. For $\zeta \neq 0$, entropy density, S , is produced; we describe this production by a generation function $G_0(\zeta)$ with $G_0(\zeta \neq 0) > 0$. Electric fields E and currents j produce entropy via the Joule heating term, jE , leading to (T is a pseudo-temperature defined later)

$$T\partial_t S = \sigma \vec{E}^2 + G_0(\zeta) = \rho j^2 + G_0(\zeta). \quad (1)$$

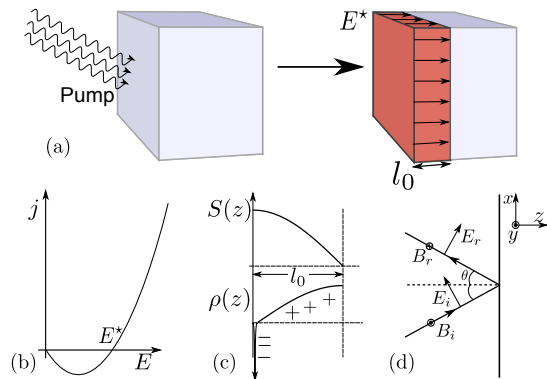


FIG. 2. (Color online) (a) Sketch of incident pump pulse leading to spontaneous polarization in the active layer. (b) Sketch of the j - E characteristic for a $\sigma < 0$ state. (c) Entropy and charge density profiles inside the active layer; notice the thin surface charge accumulation on the external boundary of the layer. (d) Incident and reflected probe waves at an angle θ ; the reflection occurs in the $x-z$ plane and the magnetic field is along the y axis for TM polarization.

Here, the conductivity (resistivity) σ (ρ) depends on ζ, T .

The second law of thermodynamics requires $\frac{dS}{dt} \geq 0$. At equilibrium $G_0(\zeta = 0) = 0$, implying $\rho \geq 0$. This means that in a system which is superconducting ($\rho = 0$ for a range of T), $\rho(T)$ cannot be an analytic function of T : in other words, the onset of a superconducting state is necessarily via a phase transition (gauge symmetry breaking). However, in non-equilibrium, $G_0 > 0$ so ρ or σ can cross zero without any non-analyticity. Indeed, calculations have found negative conductivities in several models of continuously driven systems [12–17] and other models with similar properties may exist [18].

ii) A state with $\vec{E} = 0$ and $\sigma < 0$ is unstable towards formation of domains of electric field, see Fig. 2a. To see this, we combine the continuity and Poisson equations

$$\nabla \cdot \vec{j}_D = 0; \quad \vec{j}_D = \vec{j} + (4\pi)^{-1} \partial_t \vec{D}; \quad \nabla \times \vec{E} = 0, \quad (2)$$

with the constitutive equation $\vec{j} = \sigma \vec{E}$. Here $\vec{D} = \epsilon_r \vec{E}$ is the electric displacement and ϵ_r is the electric permittivity (for simplicity we treat ϵ_r, σ as isotropic). If $\sigma < 0$, the $E = 0$ solution is unstable: small fluctuations in E (*i.e.* charge) grow exponentially with time. Then, the non-linear dependence of the current on the electric field becomes important. In particular, at some finite value of the electric field $E = E^*(\zeta)$ the Joule heating vanishes again ($\vec{E}^* \vec{j}(E^*, \zeta) \rightarrow 0$), see Fig 2b and Refs. [14, 16], implying the formation of a state characterized by domains of electric field $\sim E^*$ bounded by thin sheets of electric charge. The thickness of the sheets is determined by microscopic scales, and is not important for the physics we consider. As usual for non-linear equations, a multiplicity of possible domain structures may occur. Their detailed analysis is a formidable but often unnecessary task and they were studied extensively in several works [19].

iii) We study the physical consequences of domain formation under the main assumption that the non-

equilibrium effects are strong enough to have $\sigma(E = 0) < 0$ in some region near the sample surface, leading to the formation of a spontaneous polarization $E^*(z)$ in an *active layer* $0 < z < l_0$ [shaded region (red on-line) in the right portion of Fig. 2a]. We assume that the depth, l_0 , of this active layer and the spontaneous polarization change slowly with ζ as the system relaxes to equilibrium, and that E^* is determined by the dynamics of $\zeta(z, t)$, apart from the small fluctuations considered below.

After the pump is switched off, the microscopic degrees of freedom rapidly relax to their quasi-equilibrium values; in particular, the electric field relaxes to $E^*[\zeta(z, t)]$. Because the system is no longer driven, the total energy is conserved, so the state is characterized by three slowly evolving variables: the parameter ζ , the energy density $\varepsilon(\vec{r}, t)$, and the electric field E [connected to the charge and current densities by Eq. (2)]. The entropy density S is related to these dynamical variables by the equation of state $S(\varepsilon, \vec{D}, \zeta)$.

Conservation of energy means the energy density (which includes the electric field energy) evolves only via the energy current \vec{j}_ε

$$\partial_t \varepsilon + \vec{\nabla} \cdot \vec{j}_\varepsilon = 0. \quad (3)$$

Let us note in passing that the Joule heating increases the internal energy of the electron system but decreases the energy of the electric field so that it cancels from (3).

The time evolution of ζ depends on ε as a parameter (since for homogeneous systems ε is an integral of motion) and on ζ itself [20],

$$\partial_t \zeta = -I(\zeta, \varepsilon); \quad I(\zeta = 0, \varepsilon) = 0. \quad (4)$$

For the third dynamical equation we choose the entropy S within the active layer as the independent variable with \vec{D} determined from the equation of state:

$$(4\pi)^{-1} \vec{E} \cdot d\vec{D} = d\varepsilon - TdS + T\partial_\zeta S d\zeta. \quad (5)$$

This choice enables us to use the conservation of energy (3) effectively. The entropy evolution can be written as

$$T\partial_t S = G(\zeta, \varepsilon) > 0; \quad T^{-1} = (\partial S / \partial \varepsilon)_{\zeta, \vec{D}}. \quad (6)$$

Entropy generation arises both from Joule heating and from the entropy produced by the relaxation of ζ . The two effects cannot be separated in the non-equilibrium regime we consider and that is why they are joined in one kinetic term G . However, the ratio $G/I = -T(\partial S / \partial \zeta)_{\varepsilon, \vec{D}}$ is determined directly by the state function; it is analogous to a thermodynamic quantity and does not depend on the kinetic coefficients.

To complete the system of equations we observe that in the lowest order of the gradient expansion

$$\vec{j}_\varepsilon = -\kappa T \vec{\nabla} S, \quad (7)$$

where κ is the thermal diffusion coefficient (related to the thermal conductivity via the specific heat) [21]. The contribution of the particle current to the energy current can be neglected provided that all the relevant linear scale are much larger than the screening radius.

Equations (3)–(7) provide a complete description of the dynamics of the system in the non-relativistic limit (speed of light $c \rightarrow \infty$) and in the absence of incident radiation. It is noteworthy that Eq. (5) shows that in the situation considered here, $\vec{E} \simeq \vec{E}^*$, fluctuations of energy and entropy are linearly coupled to the electric field, in contrast to equilibrium where the linear coupling is only via Seebeck and Peltier effects which involves only spatial derivatives of the electric field.

For an isolated system $(\varepsilon_0, S_0, \zeta_0)_{(z,t)}$ slowly evolve according to Eqs. (3)–(7). Let us consider small deviations around this evolving state: we write $\varepsilon(\vec{r}, t) = \varepsilon_0(\vec{r}, t) + \delta\varepsilon$ *etc* and linearize Eqs. (3)–(7), obtaining

$$\hat{L} \begin{pmatrix} \delta\zeta \\ \delta\varepsilon \\ T\delta S \end{pmatrix} = 0; \quad \hat{L} = \begin{pmatrix} \frac{\partial}{\partial t} + \frac{\partial I}{\partial \zeta} & \frac{\partial I}{\partial \varepsilon} & 0 \\ 0 & \frac{\partial}{\partial t} & -\kappa \frac{\partial^2}{\partial z^2} \\ -\frac{\partial G}{\partial \zeta} & -\frac{\partial G}{\partial \varepsilon} & \frac{\partial}{\partial t} \end{pmatrix}, \quad (8)$$

with boundary conditions

$$\partial_z T\delta S|_{z=0} = 0, \quad \delta S|_{z=l_0} = 0. \quad (9)$$

The first boundary condition says entropy does not flow into the vacuum; the second one states that any excitation reaching the internal boundary of the active layer is removed into the bulk [22]. Notice that $\delta\varepsilon$ can be discontinuous at boundaries due to charge accumulation.

The coefficients in \hat{L} depend slowly on time, justifying the use of a quasi-stationary approximation for the response to rapidly varying perturbations (perturbation frequency $\omega \gg \frac{\partial I}{\partial \zeta}$). For simplicity we also assume that all coefficients of \hat{L} in Eq. (8) do not depend on z within the layer $0 < z < l_0$ (lifting this assumption leads to unimportant changes in numerical coefficients). We seek solutions of the form

$$\delta\zeta, \delta\varepsilon, T\delta S \sim e^{-i \int^t dt_1 \omega(t_1)} \cos(kz). \quad (10)$$

We define

$$\omega_E \equiv \partial_\varepsilon G; \quad \gamma \equiv \partial_\varepsilon I (\partial_\varepsilon G)^{-1} \partial_\zeta G, \quad (11)$$

and substitute Eq. (10) into Eq. (8), finding

$$k(\omega) = \omega / \sqrt{\kappa \omega_E (1 - i\gamma/\omega)}. \quad (12)$$

From the second boundary condition in Eq. (9) $k^j l_0 = \pi(j + \frac{1}{2})$; the lowest eigenfrequency is then:

$$2\omega_0 \approx \sqrt{\pi^2 \omega_E \kappa / l_0^2 - i\gamma}. \quad (13)$$

The frequency ω_0 will determine the scale of the non-equilibrium anomaly in the reflectivity and depends on time through ω_E and l_0 . Equation (13) shows that the active layer sustains underdamped fluctuations, originating from the combination of plasmonic charge dynamics, the relaxation of ζ and slow fluctuations of the energy. The coupling between the charge and energy/entropy fluctuations is large because charge fluctuations produce electric fields which contribute to the energy density, while even small changes in ε cause large changes in the entropy production. Other oscillations involving such quantities such as the spin density are possible, but their coupling to the entropy fluctuations will be much weaker, as the interactions with the corresponding densities are local.

We now turn to the reflectivity. Coupling the collective mode (13) to electromagnetic wave requires replacing Eq. (2) with the complete set of Maxwell equations

$$c\vec{\nabla} \times \vec{B} = 4\pi\vec{j}_D; \quad c\vec{\nabla} \times \vec{E} = -\partial_t \vec{B}, \quad (14)$$

where \vec{B} is the magnetic field (we assume permeability $\mu = 1$). The magnetic field in Eq. (14) modifies the expression for the energy current from Eq. (7) to

$$\vec{j}_\varepsilon = -\kappa T \vec{\nabla} S + \vec{\mathcal{P}}; \quad 4\pi\vec{\mathcal{P}} \equiv c\vec{E} \times \vec{B}, \quad (15)$$

where $\vec{\mathcal{P}}$ is the Poynting vector acting as an external source for the energy dynamics inside the active layer.

We consider “probe” radiation incident at an angle θ and distinguish two polarizations: when electric field $\delta E \parallel \hat{y}$ (TE polarization) or when δE has a component along z (TM polarization, see Fig. 2d). Symmetry dictates that electric fields associated with TE radiation cannot interact with the charge oscillations of the longitudinal mode Eq. (10) so that no significant changes in $R(\omega)$ may occur (the other way to see this is to notice that the Poynting vector is $\vec{\mathcal{P}} \parallel \hat{y}$ but the only important spatial variation is along x so $\vec{\nabla} \cdot \vec{\mathcal{P}} = 0$). The absence of a pump dependent correction for TE polarization is a key qualitative result of our model.

For TM polarization the Poynting vector of the incident wave indeed acts as a source in the energy conservation Eq. (3), modifying Eq. (8) to

$$4\pi\hat{L}(\delta\zeta; \delta\varepsilon; T\delta S)^T = c(\partial_x B)E^*(0; 1; 0)^T, \quad (16)$$

where the condition $\omega l_0/c \ll 1$ implies that the dependence of B on z can be neglected. The linear perturbation of the layer is maximal when the frequency of the probe is close to the real part of the frequency ω_0 [Eq. (13)].

We now calculate the frequency dependent reflectivity $R = |r|^2$ in terms of the amplitude, $r(\theta, \omega)$, of the reflected portion of a TM wave incident at angle θ :

$$r(\theta, \omega) = \left(4\pi \cos \theta - c\vec{Z}\right) / \left(4\pi \cos \theta + c\vec{Z}\right). \quad (17)$$

The total impedance $\tilde{Z}(\theta, \omega)$ is defined as

$$\frac{1}{\tilde{Z}(\theta, \omega)} \equiv \frac{c}{4\pi} \frac{B_y(z=0)}{E_x(z=0)} = \frac{\int_0^\infty j_D^x dz}{E_x(z=0)}, \quad (18)$$

where the last equation is obtained by integration of the first Maxwell equation (14) over z within the sample.

The total displacement current is given by

$$\int_0^\infty j_D^x dz = [Z_0(\theta, \omega)]^{-1} E_x(z=l_0) + \int_0^{l_0} j_D^x dz, \quad (19)$$

where $Z_0(\theta, \omega)$ is the equilibrium impedance in the bulk and the second term is always small for $\omega l_0/c \ll 1$. It is the field E_x that drastically changes across the active layer; in fact, for $\omega l_0/c \ll 1$, $\vec{\nabla} \times \vec{E} \approx 0$ and we obtain

$$E_x|_{z=l_0} - E_x|_{z=0} = \int_0^{l_0} \partial_x \delta E_z dz = \int_0^{l_0} \frac{\partial_x \delta D_z}{\epsilon_r} dz. \quad (20)$$

Finding δD_z from Eqs. (5) and (16) we obtain the angular dependence of the non-equilibrium impedance

$$\tilde{Z} = Z_0(\theta, \omega) + Z_{neq}(\theta, \omega); \quad Z_{neq} \equiv \sin^2 \theta Y(\omega), \quad (21)$$

where $Z_0(\theta, \omega)$ has to be extracted from equilibrium experimental measurements [23].

The factorization of the non-equilibrium contribution Z_{neq} into angle and frequency dependent terms is a distinctive feature of the active layer model. The specific θ -dependence shown in Eq. (21) is a consequence of the assumed domain shape. A more complex domain structure would produce a more complicated θ -dependence.

The function $Y(\omega)$ is formally expressed as

$$\frac{c}{4\pi} Y(\omega) = \frac{1}{\epsilon_r} \frac{\omega^2}{c} \int_0^{l_0} dz_1 dz_2 \frac{1}{E^*(z_1)} \mathcal{L}_{z_1, z_2} E^*(z_2); \quad (22)$$

$$\mathcal{L} = \left[(-G/I, 1, -1) \hat{L}^{-1} (0; 1; 0)^T \right].$$

We neglect the factor G/I which is of the order of the rate at which the state relaxes back to equilibrium divided by the frequency: $\frac{G}{I} \sim \frac{\partial I / \partial \zeta}{\omega} \ll 1$. Explicit calculation within the model leading to Eq. (13) gives

$$\frac{c}{4\pi} Y(\omega) = -\frac{\omega_E l_0}{\epsilon_r c} \left(1 - i \frac{\gamma}{\omega} \right) \left(\frac{\tan[k(\omega) l_0]}{k(\omega) l_0} - 1 \right), \quad (23)$$

where $k(\omega)$ is found from Eq. (12). The function $Y(\omega)$ (see Fig. 3a) vanishes as $\omega \rightarrow 0$. For small ω , $\text{Re}(Y) < 0$ and Y has poles at the eigenfrequencies given in Eq. (13). The high frequency behavior cannot be obtained from Eq. (23), valid only for $\omega < \frac{c}{l_0}$. The remarkable feature of Eq. (23) is that the pre-factor ($\omega_E l_0/c$) can easily exceed unity; the origin of this largeness is the sensitivity of the entropy production to the integral of motion ε .

We used Eqs. (17), (21), (23) to calculate the reflectivity.

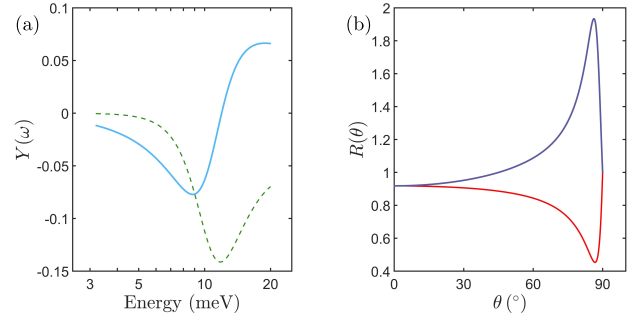


FIG. 3. (Color online) (a) Plot of the real (solid line) and imaginary (dashed line) part of $Y(\omega)$. (b) Theoretical $R(\theta)$ of K_3C_{60} at $\omega = 6 \text{ meV} = 1.44 \text{ THz}$ in equilibrium (red) and non-equilibrium (blue); notice the marked dependence on the angle and the presence of a region where $R > 1$. Plots are for the parameters of Fig. 1a.

From Eq. (21) we see that at $\theta = 0$ (normal incidence) the non-equilibrium effects are not visible in R , while from Eq. (17) we see that at $\theta = \pi/2$, $|r| = 1$ for both equilibrium and non-equilibrium states. For $0 < \theta < \pi/2$, non-equilibrium effects are evident in the reflectivity, see Fig. 3b. Intuition may be gained considering the Hagen-Rubens limit $|\tilde{Z}| \ll 1$ [24] in which $R(\omega) \approx 1 - 4\text{Re}[Z_0 + \sin^2 \theta Y(\omega)] / \cos \theta$, showing that the reflectivity is enhanced relative to equilibrium for $Y < 0$ and suppressed for $Y > 0$. The large value of $\omega_E l_0/c$ means that $\text{Re}(Z)$ can become *negative* for $\omega \lesssim \text{Re}(\omega_0)$, leading to $R > 1$; such amplification is allowed in a non-equilibrium system. Notice however that in there is no spontaneous emission instability (no lasing).

We briefly mention nonlinear response effects implied by our model: (i) Second harmonic generation (SHG) is made possible by the non-zero value of the spontaneous polarization E^* , which reduces the symmetry to uniaxial. The SHG signal is maximal for excitation frequencies near $\omega_0/2$ and ω_0 , corresponding to resonances in the outgoing or incoming state respectively. (ii) A parametric resonance instability may lead to radiation at frequencies $\sim \omega_0$ in response to an incident wave of frequency close to $2\omega_0$ [25]; the observable features are the same as those of the recently discussed “Floquet time crystal” state [26].

In conclusion, we plotted $R(\omega) = |r(\omega, \theta = 45^\circ)|^2$ for “sensible” parameters values in Figs. 1a and 1b. The resemblance with the experimental data is very reasonable, even though we cannot make any definite conclusion until the data on polarization and angular dependence are available.

We are grateful to A. Andreev, D. Basov, A. Cavalleri, M. Dyakonov, Y. Galperin, A. Georges, and L. Glazman for helpful discussions of the results of this paper. Support was provided by the Basic Energy Sciences Division of the U.S. DOE grant DE-SC0018218 (A.M. and G.C.) and by the Simons Foundation (I.A.).

-
- [1] R. D. Averitt and A. J. Taylor, *Journal of Physics: Condensed Matter* **14**, R1357 (2002).
- [2] M. Mitrano, A. Cantaluppi, D. Nicoletti, S. Kaiser, A. Perucchi, S. Lupi, P. Di Pietro, D. Pontiroli, M. Riccò, S. R. Clark, D. Jaksch, and A. Cavalleri, *Nature* **530**, 461 (2016).
- [3] D. Nicoletti, E. Casandruc, Y. Laplace, V. Khanna, C. R. Hunt, S. Kaiser, S. S. Dhesi, G. D. Gu, J. P. Hill, and A. Cavalleri, *Phys. Rev. B* **90**, 100503 (2014).
- [4] D. Fausti, R. I. Tobey, N. Dean, S. Kaiser, A. Dienst, M. C. Hoffmann, S. Pyon, T. Takayama, H. Takagi, and A. Cavalleri, *Science* **331**, 189 (2011).
- [5] D. M. Kennes, E. Y. Wilner, D. R. Reichman, and A. J. Millis, *Nature Physics* **13**, 479 (2017).
- [6] M. Knap, M. Babadi, G. Refael, I. Martin, and E. Demler, *Phys. Rev. B* **94**, 214504 (2016).
- [7] M. A. Sentef, A. F. Kemper, A. Georges, and C. Kollath, *Phys. Rev. B* **93**, 144506 (2016).
- [8] J. I. Okamoto, A. Cavalleri, and L. Mathey, *Phys. Rev. Lett.* **117**, 227001 (2016).
- [9] A. Nava, C. Gianetti, A. Georges, E. Tosatti, and M. Fabrizio, *Nature* **14**, 154 (2018).
- [10] Y. Lemonik and A. Mitra, *cond-mat/1804.09280* (2018).
- [11] M. Kim, Y. Nomura, M. Ferrero, P. Seth, O. Parcollet, and A. Georges, *Phys. Rev. B* **94**, 155152 (2016).
- [12] A. L. Zakharov, *Zh. Eksp. Teor. Fiz.* **38**, 665 (1960), [*Sov. Phys. JETP*, **11**, 478 (1960)].
- [13] V. I. Ryzhii, *Fiz. Tverd. Tela* **11**, 2577 (1970), [*Sov. Phys. Solid State*, **11**, 2078 (1970)]; V. I. Ryzhii, R. A. Suris, and B. S. Shchamkhalova, *Fiz. Tekh. Poluprovodn* **20**, 2078 (1986), [*Sov. Phys. Semiconductors*, **20**, 1289 (1986)].
- [14] A. V. Andreev, I. L. Aleiner, and A. J. Millis, *Phys. Rev. Lett.* **91**, 056803 (2003).
- [15] A. C. Durst, S. Sachdev, N. Read, and S. M. Girvin, *Phys. Rev. Lett.* **91**, 086803 (2003).
- [16] M. I. D'yakonov, *Pis'ma Zh. Eksp. Teor. Fiz.* **39**, 158 (1984), [*JETP Lett.*, **39**, 185 (1984)]; M. I. D'yakonov and A. S. Furman, *Zh. Eksp. Teor. Fiz.* **87**, 2063 (1984), [*Sov. Phys. JETP*, **60**, 1191 (1984)].
- [17] I. A. Dmitriev, M. G. Vavilov, I. L. Aleiner, A. D. Mirlin, and D. G. Polyakov, *Phys. Rev. B* **71**, 115316 (2005).
- [18] Existing calculations identify two origins of the negative conductivity: the photovoltaic effects [13, 15, 16] on the impurity collision process, and the distribution function effects [17]. In slowly relaxing non-driven systems only the latter effects are relevant.
- [19] See e.g. E. Schöll, *Nonlinear Spatio-Temporal Dynamics and Chaos in Semiconductors* (Cambridge University Press, New York, 2001); A. F. Volkov and S. M. Kogan, *Sov. Phys. Usp.* **11**, 881 (1969); B. W. Knight and G. A. Peterson, *Phys. Rev.* **155**, 393 (1967).
- [20] Note that ζ can always be chosen in such a way that the right hand sides of Eqs. (4) and (6) do not depend on S .
- [21] Strictly speaking Eq. (7) implies the presence of the divergence of the entropy current $\vec{j}_S = -\kappa \vec{\nabla} S$ in the LHS and of terms $\sim (\vec{\nabla} S)^2$ contributing to entropy production in the RHS of Eq. (6). Both these terms are negligible in the studied regime $\omega \gg \kappa/l_0^2$.
- [22] It can be checked that this assumption is justified for $\omega \gg \kappa/l_0^2$, which corresponds to a very small penetration length of the entropy current inside the bulk.
- [23] For K_3C_{60} we computed the impedance Z_0 using $\epsilon_r = 1.6$, $\sigma_1(\omega)/\sigma_0 = 0.12 + 0.8\sqrt{4\log^2(\omega/10) + 0.1^2}$ for $\omega < 10$ and $\sigma_1(\omega)/\sigma_0 = 0.2$ for $\omega > 10$, $\sigma_2(\omega)/\sigma_0 = 2/3 - 1.98\log^2(\omega/3)$ for $\omega < 8$ and $\sigma_2(\omega)/\sigma_0 = 1/30 - 1.98\log^2(\omega/20)$ for $\omega > 8$, where $\sigma_0 = 400\Omega^{-1}\text{cm}^{-1}$ and ω is expressed in meV. This choice of σ reproduces the important low frequency features of the reflectivity in Fig. 2a of Ref. [2]. For LBCO we reproduced the equilibrium data from Fig. 2b.2 of Ref. [3] using $\sigma = 3.5\Omega^{-1}\text{cm}^{-1}$ and $\epsilon_r = 50$.
- [24] E. Hagen and H. Rubens, *Ann. d. Physik* **4**, 873 (1903).
- [25] See e.g. § 27, 28 of L. D. Landau and E. M. Lifshitz, *Mechanics (Course of theoretical physics; v.1)*, 3rd ed. (Elsevier, London, 1976).
- [26] D. V. Else, B. Bauer, and C. Nayak, *Phys. Rev. Lett.* **117**, 090402 (2016).